AIMS Biophysics

AIMS Biophysics, Volume (Issue): Page.
DOI:
Received:
Revised:
Accepted:
Published:

http://www.aimspress.com/journal/biophysics

Research article

Firing patterns and network dynamics of an extended Hindmarsh-Rose neuronal system

Yan Fu[1], Guowei Wang [2,*]

[1] School of Mathematics & Computer Science, Yuzhang Normal University, Nanchang, 330103, China
[2] School of Education, Nanchang Institute of Science & Technology, Nanchang, 330108, China

* **Correspondence:** guoweiwang@mails.ccnu.edu.cn.

Abstract: The analysis of Hindmarsh-Rose (HR) neural model and its network dynamics under the influence of different stimulus inputs or network topologies are the leading research edge of the structural dynamics of complex networks, but the typical three-variable HR neural model has limitations in describing the complex non-linear features and precise behavior patterns of neuron. Based on an extended HR neural model, its firing patterns and bifurcation behavior with different stimulus are analysed, and how the newly introduced variable affect discharge modes has also been explored. A two-dimensional lattice is constructed to study the mechanism of spiral wave formation and breakup in the neural network, and to explore its network dynamics and synchronous behavior. The obtained results show that the extended HR neural model has more rich and stable firing properties, and it can be observed that there are multimodal phenomena with both spiking and bursting states simultaneously. If the network topology is changed, the formation and breakup of spiral waves can be observed, and the synchronization factor exhibits a monotonically decreasing relationship with the coupling strength and the control parameters of the newly introduced variable, indicating that the changing law of the synchronization properties in the two-dimensional network can reveal the transition mechanism of the chaotic and ordered states of the network. When HR neurons are in spiking state, the system is more prone to spiral waves, and the coupling strength range for spiral waves is wider. The above results provide valuable ideas to explore the modulation of network group behavior and provides useful information for the treatment of epilepsy.

Keywords: Hindmarsh-Rose neural model; Topology; Spiral wave; Multimodality; Discharge

1. Introduction

Scientific research has shown that the nervous system of an organism is mainly composed of neurons and glia, among which neurons are the basic units of the structure and function of the nervous system [1]. The establishment of neuron theory in 1909 provided strong supported for the development of neuroscience, and humans recognized that neurons are the most fundamental way to understand and explore the nervous system [2]. Due to the unique structure of neurons, they have a high degree of asymmetry, which enables them to complete specialized tasks in the process of information transmission and processing [3]. The electrical activity of the nervous system presents complexity, and different discharge modes are switched by applying appropriate external stimuli [4]. The connection of neurons in complex network helps to achieve different collective behaviors [5].

Pattern dynamics is an important branch in the field of nonlinear science, with the aim of exploring the basic laws of the formation and evolution of patterns that exist together among various systems in the objective world and have universal guiding significance [6]. Previous studies have shown that neurons in the cerebral cortex are mainly composed of excitatory pyramidal neurons and inhibitory Interneuron [7]. The two kinds of neurons modulate the individual electrical activity of neurons through different feedback circuits, so as to ensure the normal processing and coding of neural information [8]. So the transmission of neural signals in neural networks is also a research frontier and has practical significance [9]. For neural networks, external excitation in local regions can suppress spatiotemporal chaos and spiral waves in the network [10]. In addition to random boundary values, target waves or pulses can also be generated due to the heterogeneity and parameter diversity of local regions [11]. Some biological experiments have confirmed the presence of spiral waves in the cerebral cortex, which can regulate the collective behavior of neurons [12].

Rich and diverse patterns can be observed in excitable media, and the selection of patterns in spatiotemporal systems is related to self-organizing behavior [13]. Khouhak et al. studied a 2-dimensional network of interacting nephrons by considering a local linear coupling [14]. Weise et al. identified a mechanism for mechanical wave break in the heart muscle by using a reaction-diffusion-mechanics model [15]. Jakubith et al. observed a large variety of spatiotemporal patterns depending on the applied conditions dynamics of reaction-diffusion systems [16]. Sandeep et al. demonstrated the excitation of spiral waves in the context of driven two-dimensional dusty plasma at particle level by using molecular-dynamics simulations [17]. He et al. investigated the spatiotemporal behaviour of the discrete neuron model in single- and two-layer network [18]. Rajeshkanna et al. introduced the fractional-order gene map model and investigated the system’s dynamic behaviors according to system parameters and derivative order [19]. Zhdanov et al. presented the spatiotemporal aspects of the interplay of cancer and the immune system [20]. The research on these spiral wave problems is widely found in various biological system and excitable media, and provides theoretical guidance and support for solving various problems [21].

The electrical activity of the nervous system presents complexity, and the formation and breakup of spiral waves can also be observed by changing external stimuli or network topology [22]. In many cases, spiral waves in the nervous system may be closely related to various diseases, so people attach great importance to spiral wave patterns in neural networks [23]. Shepelev et al. investigated Synchronization of wave structures in a heterogeneous multiplex network of 2D lattices with attractive and repulsive intra-layer coupling [24]. The dynamics of a two-dimensional ensemble of nonlocally coupled van der Pol oscillators is studied by Bukh [25] et al. The elimination of spiral waves is

numerically studied by Etémé et al. in a network of Hindmarsh-Rose neurons in presence of long-range diffusive interactions and external frequency excitations in 2019 [26]. Nayak et al. carried out an extensive numerical study of the dynamics of spiral waves of electrical activation in the presence of periodic deformation in two-dimensional simulation domains [27]. Bukh et al. investigated numerically the spatio-temporal dynamics of a 2D lattice of coupled discrete-time systems with nonlocal interaction [28]. Wu et al. studied the pattern formation induced by gradient field coupling in bi-layer neuronal networks [29]. Yao et al. carried out the impacts of bounded noise and rewiring of network on the formation and instability of spiral waves in small-world network of Hodgkin-Huxley neurons through numerical simulations [30]. Wang et al. analysed the spatiotemporal patterns and collective dynamics of bi-layer coupled Izhikevich neural networks with multi-area channels [31]. Luo et al. proposed a new modified Fitzhugh-Nagumo model and studied the dynamic behaviors of spiral waves in cardiac tissue under fixed or periodic electromagnetic radiation [32].

Hindmarsh and Rose conducted extensive experiments on the visceral ganglia of pond snails, and they proposed a bi-variate neuronal model in experimental observations in 1982 [33]. In the following research, they found that this model could not explain the phenomenon of neuronal bursting discharge, and then they made modifications to the model and obtained the famous HR neuronal model [34]. Due to the rich discharge characteristics of the HR model, a large number of researchers have conducted extensive research on it [35]. Xu et al. investigated the of emergence of target wave and spiral wave in neuronal network induced by gradient coupling in HR neural model [36]. Ma et al. designed a forward feedback neuronal network in chain type and described the local kinetics for each node by HR neuron [37]. Torrealdea et al. deduced an energy function for a HR neuron model and used it to evaluate the energy consumption of the neuron during its signaling activity [38]. In our previous research work, we studied the modes transition and network synchronization in extended HR model driven by mutation of adaptation current under effects of electric field [46]. These studies have done a lot of meaningful work and provided very valuable guidance for computational neuroscience, but there is still a problem that has been ignored in previous studies.

As we all know, the HR neural model can not only facilitate computation, but also generate most of the discharge behaviors exhibited by real biological neurons, such as quiescence, spike discharge, and burst discharge. However, the three-variable HR neuronal model has one clear drawback. When it comes to complex nonlinear problems of neuron or when describing the precise behavior patterns of neurons, the classic three variables HR neuronal model shows certain limitations. Considering the above reasons, the impact of newly introduced variables on their firing patterns and bifurcation have not been analyzed yet. Moreover, the spatiotemporal dynamics in the two-dimensional lattice constructed by extended HR neural model have not been reported, and it is also unclear how the control parameters in the newly introduced variable regulate the formation and breakup mechanism of spiral waves in the two-dimensional lattice network. Therefore, the above issues deserve careful exploration.

In this paper, the firing patterns and bifurcation behavior of the extended HR neural model with different stimulus inputs are analysed firstly. Based on the characteristics of the control parameter in the newly introduced variable, the influence of the control parameter on the discharge modes and bifurcation are discussed, respectively. A two-dimensional lattice is constructed using random boundary functions and no-flow boundary conditions to explore the formation and breakup mechanisms of spiral waves in the neural network, and the mechanism of how the various parameters regulate the synchronization properties of networks is also explored.

The rest of the present paper is organized as follows. In Section 2, the models and methods is

proposed. We give out an extended four-variable HR neuronal model and construct a two-dimensional neural network. Section 3, we analyze the firing patterns and bifurcation of the extended four-variable HR neuronal model. Formation and breakup of the spiral waves and the synchronization factor of the network are investigated. The conclusion is given in Section 4.

2. Models and Methods

2.1. Three-Variable Hindmarsh-Rose Neuronal Model

The classical HR neuron model was proposed by Hindmarsh and Rose in 1982 [33]. This model was simplified to obtain a system of equations including 3 dimensions, and its main modeling objects were derived from snail neurons and thalamic neurons [39]. The three-variable HR neuronal model is described by the equations as follows [40].

$$\left.\begin{aligned} \frac{dx}{dt} &= y - ax^3 + bx^2 - z + I_{ext}; \\ \frac{dy}{dt} &= c - 5x^2 - y; \\ \frac{dz}{dt} &= r(s(x + 1.56) - z); \end{aligned}\right\} \tag{1}$$

where x represents the membrane potential of the neuron, y represents the recovery fast variable, z is defined as the adaptive slow current, and *Iext* indicates the input stimulus [41]. Other parameters are selected as $a = 1$， $b = 3$， $c = 1$， $r = 0.006$ and $s = 4$.

2.2. Extended Four-Variable Hindmarsh-Rose Neuronal Model

With the deepening of scientific research, the classic three variable HR neural model has also shown certain flaws 41. For example, it shows certain limitations when it comes to the complex nonlinear problems of neurons or to describe the precise behavioral patterns of neurons 42. In order to solve the above problems, the researchers creatively proposed an improved extended HR neural model, by introducing a new variable w to describe the slow exchange of calcium ions between the cytoplasm and its storage medium, so as to solve the problem better 43. The extended four-variable HR neuronal model can be described by the following equations 44.

$$\left.\begin{aligned} \frac{dx}{dt} &= y - ax^3 + bx^2 - z + I_{ext}; \\ \frac{dy}{dt} &= c - 5x^2 - y - (1/k)w; \\ \frac{dz}{dt} &= r(s(x + 1.56) - z); \\ \frac{dw}{dt} &= d(-w + e(y + 0.9)); \end{aligned}\right\} \tag{2}$$

where $d = 0.0002$, $e = 0.88$, $1/k$ represents the control parameter related to the calcium ion exchange rate, and its commonly used value is $k = 80$ 45.

149 *2.3 Two-Dimensional Neural Network*

150 A two-dimensional $N\times N$ ($N = 110$) neural network is constructed, and all the neurons are arranged
151 regularly in the way of lattice to form a square network in the two-dimensional plane 46. The no-flow
152 boundary conditions are considered at the boundary positions of the two-dimensional neural network,
153 and the random functions are applied on the network 47. The random boundary functions are separately
154 denoted as $x_0=0.8\alpha\ln(i)-0.2\alpha\ln(j)-3$, $y_0=-0.8\alpha\ln(i)+0.2\alpha\ln(j)-5$, $z_0= 0.8\alpha\ln(i)-0.2\alpha\ln(j)-1$,
155 $u_0=-0.8\alpha\ln(i)+0.2\alpha\ln(j)-5$, where α represents a random number between 0 and 1. The no-flow
156 boundary condition assumes that the values inside and outside the boundary are equal, i. e., the values
157 outside the boundary are set the same as the values within the boundary, so the inflow into the network
158 is zero, therefore it is called no-flows boundary 55. Since the coupling current in the two-dimensional
159 neural network is zero, the spiral wave production is directly related to the random boundary values
160 48. The connectivity method for this network is represented as follows.

$$\left.\begin{aligned}
\frac{dx_{i,j}}{dt} &= y_{i,j} - ax_{i,j}^3 + bx_{i,j}^2 - z_{i,j} + I_{ext,i,j} + D_{i,j}(x_{i,j-i} + x_{i,j+i} + x_{i-1,j} + x_{i+1,j} - 4x_{i,j});\\
\frac{dy_{i,j}}{dt} &= c - 5x_{i,j}^2 - y_{i,j} - (1/k)w_{i,j};\\
\frac{dz_{i,j}}{dt} &= r(s(x_{i,j} + 1.56) - z_{i,j});\\
\frac{dw_{i,j}}{dt} &= d(-w_{i,j} + e(y_{i,j} + 0.9));
\end{aligned}\right\} \quad (3)$$

162 where the subscripts i and j represent the spatial position of the neurons, which can also be called nodes
163 (i, j).

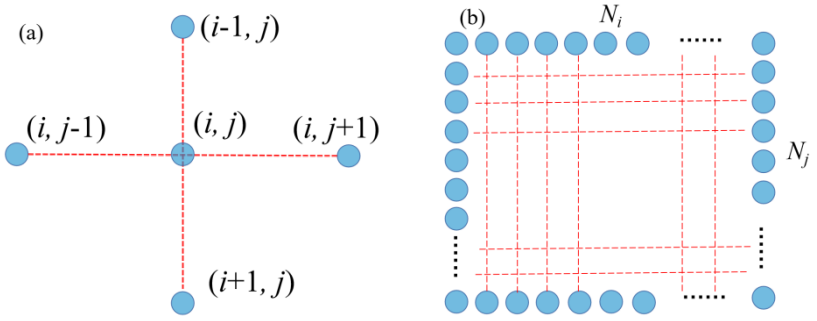

164

165 **Figure 1.** (a)Schematic of neuron coupling connection; (b)Schematic of $N\times N$ two-dimensional
166 lattice.

167 As it can be seen from Figure 1, any neuron (i, j) is connected to other neurons in four positions,
168 marked as upper $(i-1, j)$, lower $(i+1, j)$, left $(i, j-1)$ and right $(i, j+1)$, and the coupling strength between
169 neurons is D 49.

170 *2.4 Synchronization Factor*

171 The mean-field theory shows that the synchronization factors are generally introduced as the
172 statistics to describe the collective behavior and phase synchronization of the neurons when studying
173 the synchronization dynamics of the collective behavior of a large number of neurons 53. The

synchronization factor is expressed by R, and its specific calculation method is as follows 51.

$$\left.\begin{aligned} F &= \frac{1}{N^2}\sum_{j=1}^{N}\sum_{i=1}^{N} x_{i,j} \\ R &= \frac{\left\langle F^2 \right\rangle - \left\langle F \right\rangle^2}{\frac{1}{N^2}\sum_{j=1}^{N}\sum_{i=1}^{N}\left(\left\langle x_{i,j}^2 \right\rangle - \left\langle x_{i,j} \right\rangle^2\right)} \end{aligned}\right\} \tag{4}$$

where N represents the number of neurons' connected nodes in the neural network, and < > represents the statistical mean of a certain computed parameter 57. According to the existing experience, if the synchronization factor is small ($R \to 0$), the synchronization state of the system is poor. If the synchronization factor tends to 1 ($R \to 1$), the synchronization state of the system is good 50.

3. Discussion and Analysis

In order to study the discharge modes and bifurcation behavior of extended HR neuronal model under different external input conditions in detail, the Euler method was used to calculate the neuronal membrane potential, and the C++ software was used to build the neural network 错误!未找到引用源。. The Origin software was used to simulate and quantitatively analyze the generated membrane potential, bifurcation diagram (*ISI*), spiral wave patterns and network synchronization 55.

3.1 Firing patterns and Bifurcation

Select appropriate parameters and set the time step as 0.001 to simulate and analyze the above equations 错误!未找到引用源。. When the intensity of external input stimulus is changed, the bifurcation of membrane potential of the HR and extended HR neuronal models are shown in Figures 2(a) and 2(b), respectively. The bifurcation diagram is plotted by calculating the Inter-Spike Interval(*ISI*) of membrane potential 57.

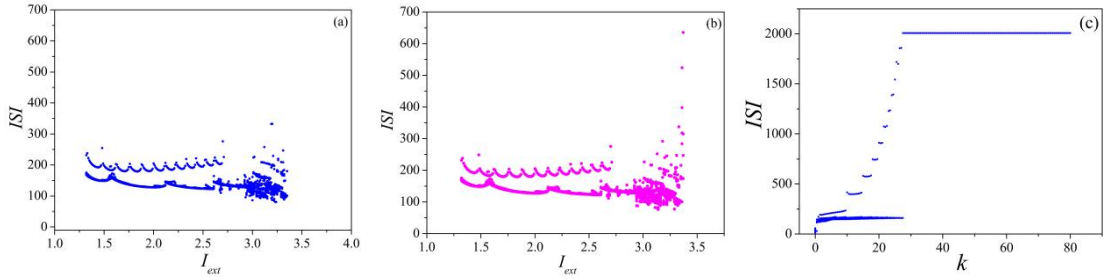

Figure 2. Bifurcation of membrane potential under different conditions. (a)*ISI* verse *Iext* of HR model; (b)*ISI* verse *Iext* of extended HR neural model; (c)*ISI* verse *k* of extended HR neural model.

It can be seen from Figures 2(a) and 2(b) that when the intensity of external stimulation current increases, the firing pattern of neuronal model undergoes changes in quiescent state, bursting, spiking, and chaos states, etc. However, it is worth noting that, when the new variable w is introduced into the HR model to describe the slow exchange of calcium ions between the cytoplasm and its storage medium, the discharge patterns of the extended HR neuronal model become more diverse, especially when the current is relatively high. Figure 2(c) shows the bifurcation diagram of the extended HR neuronal model when the control parameter k changes, and it can be clearly seen that the *ISI* presents

a stepped shape. When the value of k is less than 10, there are always some smaller values in the time interval of membrane potential, which means there exists bursting states. As the value of k increases, the form of bursting changes, and the *ISI* also correspondingly increases, showing a stepwise upward trend. If the value of k is greater than 30, the neuron exhibits a spiking discharge pattern. From the above results, it can be concluded that both external current and control parameter k have significant effects on the firing modes of HR neural model.

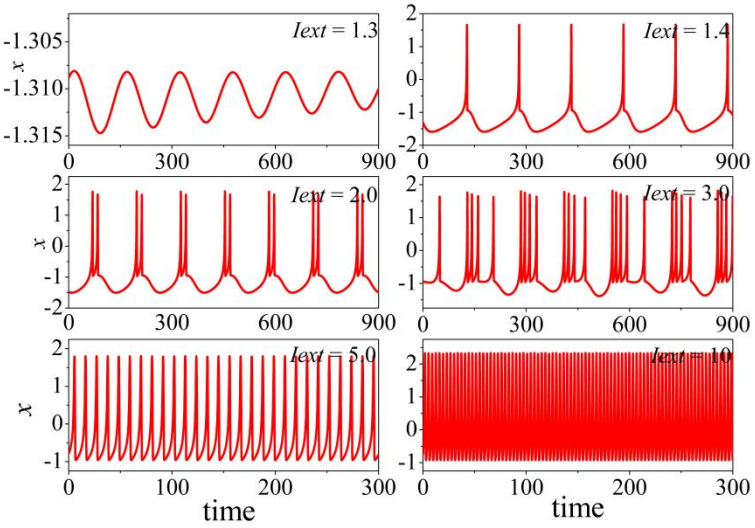

Figure 3. Membrane potential of extended HR neural model with different external stimulus intensities. With the increase of external stimulation current, one can sequentially observe firing modes such as spiking and period bursting, and the appearance of multimodal discharge can be observed.

If the external current intensity is changed, the extended HR neuronal model also exhibits rich discharge patterns, as shown in Figure 3. Consistent with the *ISI* image in Figure 2(b), if the intensity of external stimulation is less than 1.4, the extended HR neural model is in quiescent state, which means that the membrane potential of the neuron oscillates attenuatedly under the threshold. During the process of increasing external stimulation current, spiking, period bursting, and fast spiking states can be observed in sequence. Specifically, when the external stimulus current intensity is 3.0, a multimodal presence with both spiking and bursting can also be observed, and the bursting also has various forms.

In order to understand the influence of the control parameter k of the newly introduced variable w on HR neuronal model, the time series of membrane potential under different k values are plotted in Figure 4. It can be seen clearly from Figure 4 that if the value of k is relatively small, the firing patterns of extended HR neuronal model exhibit period-2 bursting state. Increasing the value of k to 5 can observe a slight increase in the interval between peaks. Continuing to increase the value of k, it can be observed that both spiking and bursting can be observed simultaneously, which is a multimodal phenomenon. For the classic three-variable HR neuronal model, multimodal existence cannot be observed in this case.

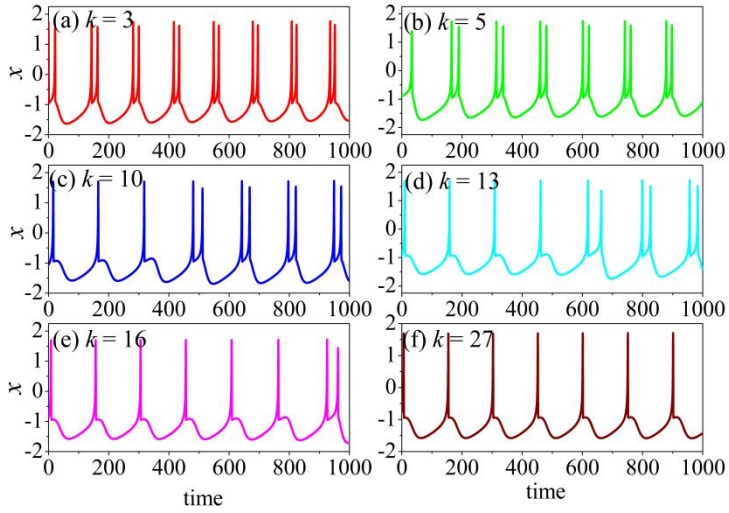

Figure 4. Membrane potential of extended HR neural model with different parameter k. The control parameter k has a significant impact on the neuronal discharge modes, and an increase in k leads to the loss of bursting state and ultimately evolve into spiking state, one can observe multimodal phenomenon when the appropriate k value is selected.

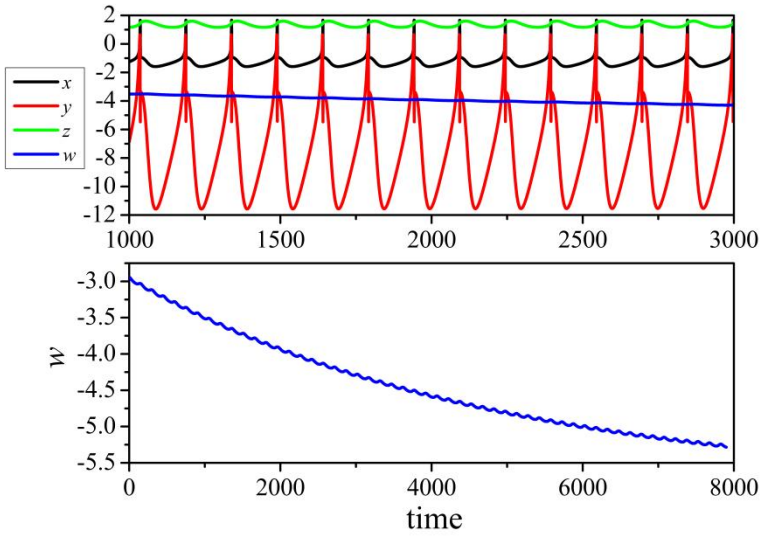

Figure 5. Time series of variables of extended HR neural model. The newly introduced variable w is used to describe the slow exchange of calcium ions between the cytoplasm and its storage medium, it exhibits a trend of oscillation attenuation over time.

In order to further investigate the impact of the newly introduced variable (i.e., the control parameter k) on the firing patterns of the extended HR neural model, the relationship between the four variables is plotted in Figure 5. It can be clearly seen from Figure 5 that the extended HR neural model is in spiking state, and the rate of change of variable y is very fast, assuming the role of rapid recovery of current. The variation of variable z is relatively slow, playing a role in slow recovery current. The newly introduced variable w is used to describe the slow exchange of calcium ions between the cytoplasm and its storage medium, it exhibits a trend of oscillation attenuation over time.

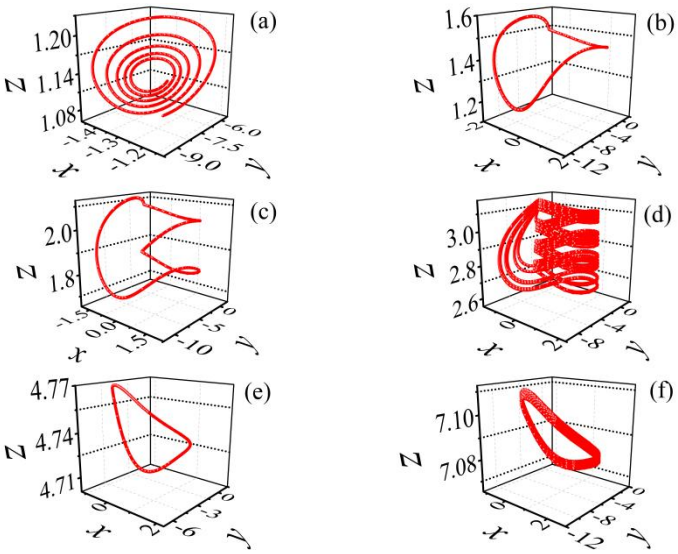

Figure 6. Phase diagram of variables of extended HR neural model. (a)-(f)**:** *Iext* = 1.3, 1.4, 2.0, 3.0, 5.0, 10.0. As the external current intensity increases, spiking, period-2 bursting, and period-4 bursting can be observed in sequence. Relatively high current intensity can lead to fast spiking patterns.

The phase diagram of variables x, y and z of extended HR neural model is plotted in Figure 6 for the sake of further exploring the characteristics of its firing patterns. When the intensity of external stimulation current is less than 1.4, the membrane potential oscillates under the threshold, and the amplitude of oscillation gradually decreases. Therefore, the phase diagram we see is an unclosed curve, presenting a continuous circular shape with gradually decreasing radius. In the following figures (for I_{ext} = 1.4, 2.0 and 3.0), spiking, period-2 bursting, and period-4 bursting can be observed in sequence. By further increasing the intensity of external stimulation current, the discharge mode evolves into spiking, and as the current intensity increases, the firing frequency increases.

3.2 Formation and breakup of the spiral waves

As is well known, spiral waves have been observed in both excitable and general media. In order to understand the mechanism how the spiral waves are generated in extended HR neuronal system, Figure 7 shows the development of spiral waves induced by random values of boundary at different external stimulus intensities with coupling strength D = 0.5. The observation time is scheduled to be 20000 unit times, the observed spiral wave pattern is basically consistent with what is expected. If the external stimulation current intensity is less than 1.3, most of the neurons are in resting states. Due to the induced effect of random boundaries, only a few neurons appear membrane potential oscillation on the boundary of the two-dimensional network.

Continuing to increase the external stimulus intensities, it can be observed that the change in external stimulus intensities has a significant modulation effect on the induction of spiral waves, resulting in multiple sets of spiral waves. The mechanism is that the induced traveling waves will be interrupted at the boundary during propagation due to the differences in the strength of random boundary effects in adjacent different regions, thereby inducing new spiral waves. Figures 7(a)-(d) tell us the potential mechanism of how spiral waves are generated, that is, the forward propagating traveling waves originate from the four boundaries of a two-dimensional network, and then collide in the central region of the network, allowing for the observation of rich spiral wave patterns. In Figure

7(d), the two-dimensional network is occupied by spiral waves, with the centers of the four sets of spiral waves approaching the four corners of the two-dimensional network, and the center of the network becoming the squeezed area.

As the external stimulus intensities increases, this interaction further increases, and the spiral wave pairs and spiral wave seeds in the network disappear, as shown in Figure 7(e). However, symmetric spiral wave pairs originating from four angles of the network were observed in Figure 7(f), and then they disappear again if the external stimulation current intensity are 2.0, 2.1, and 2.2, respectively. In Figure 7(j), it can be observed that two colliding spiral waves are entangled together. The main reason is that increasing the external stimulus intensities increases the number of peaks in neuronal bursting discharge, thickens the spiral wave arm, and increases the size of spiral waves, finally the number is correspondingly smaller. In this way, individual spiral waves can be seen in the two-dimensional network. So it can be concluded that selecting the appropriate external stimulus intensities can result in a single spiral wave, and usually multiple spiral waves and spiral wave pairs interact to cause regular or irregular patterns to appear repeatedly in the system.

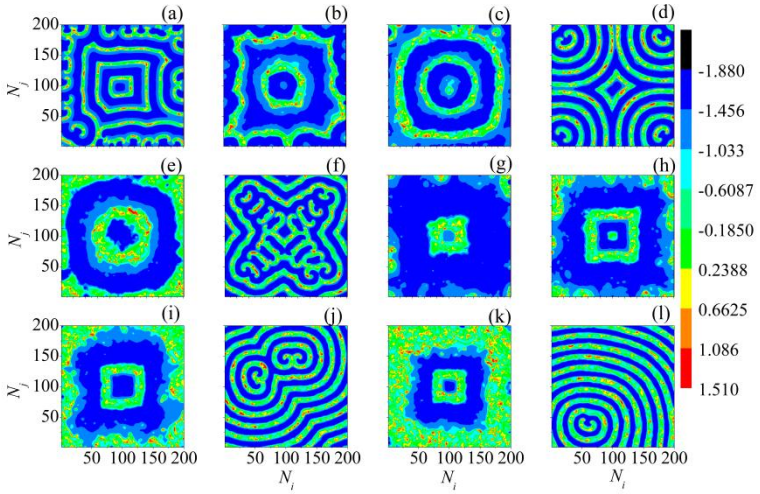

Figure 7. Development of spiral wave induced by random values of boundary at different external stimulus intensities with $D = 0.5$ at $t = 20000$ time units. (a)-(l): $I_{ext} = 1.3$, 1.5, 1.6, 1.8, 1.9, 2.0, 2.1, 2.2, 2.3, 2.4, 2.5, 2.8. The forward propagating traveling waves originate from the four boundaries of a two-dimensional lattice, and then collide in the central region of the network, allowing for the observation of rich spiral wave patterns.

As shown in Figure 8, the formation and breakup of spiral waves can also be observed when the coupling strength between adjacent neurons changes. Here, the stimulus current is chosen as $I_{ext} = 1.3$ under the threshold and the system rely on the interaction of random boundaries to excite spiral waves. When the coupling strength is selected as $D = 0.1$, a large number of neurons are in quiescent state, and the entire network has neither spiral wave seeds nor spiral waves. As the coupling strength increases, spiral wave pairs and double-armed spiral wave seeds begin to appear in the two-dimensional network. However, no matter how the coupling strength changes, a separate spiral wave pattern cannot be observed in the network. The mechanism behind this phenomenon is related to the firing patterns of neurons. That is, if the number of spiking discharges in neurons is small, the wave arm of the spiral wave is thinner, so the size of the spiral wave is small while the number is large, and there is no single spiral wave in the system. These results indicate that the probability of a single spiral wave appearing in the system is relatively low, and the probability of a small spiral wave appearing is

relatively high. These results are consistent with the experimental observations.

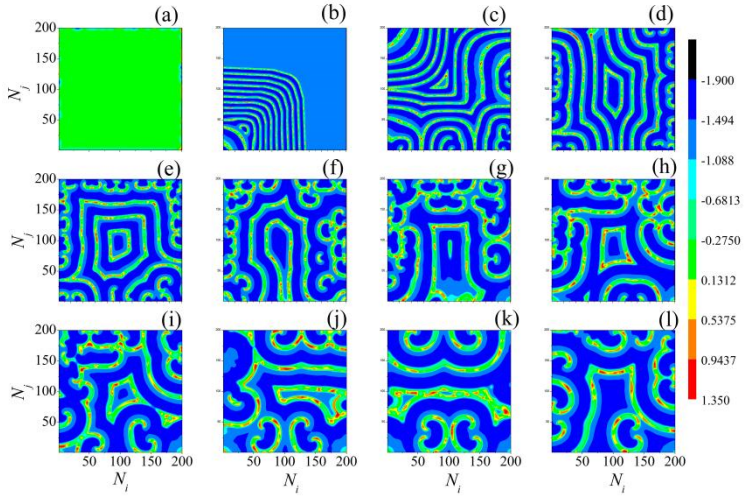

Figure 8. The development of spiral wave induced by random values of boundary at different coupling intensities D with $I_{ext} = 1.3$ at $t = 20000$ time units. (a)-(i) $D = 0.1, 0.2, 0.3, 0.4, 0.5, 0.6, 0.7, 0.8, 0.9, 1.0, 1.1, 1.2$. By changing the coupling strength between neurons, neurons below the threshold can be stimulated to start firing, thereby inducing the generation of spiral waves.

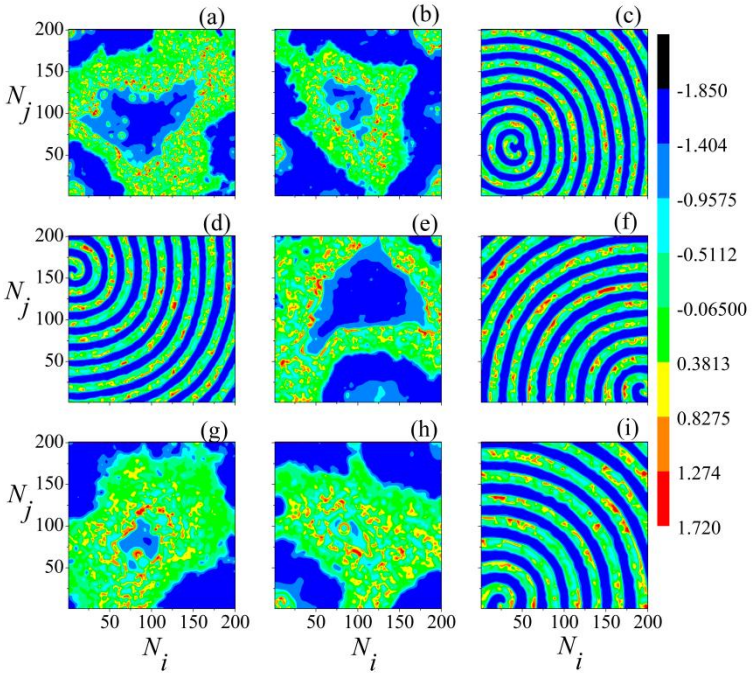

Figure 9. Development of spiral wave induced by random values of boundary at different coupling intensities D with $I_{ext} = 2.8$ at $t = 20000$ time units. (a)-(i) $D = 0.3, 0.4, 0.5, 0.6, 0.7, 0.8, 0.9, 1.0, 1.1$. No matter how the coupling strength is changed, only circular or annular waves appear, and the wave heads of these circular waves are also constantly changing.

When a larger stimulus current $I_{ext} = 2.8$ is selected, one can observe completely different results, as shown in Figure 9. It is surprised to find that only chaotic states and single spiral waves appear in case of $I = 2.8$ no matter how the coupling strength is changed, and spiral wave seeds cannot be observed. If strictly speaking, these spatiotemporal patterns cannot be called spiral waves, a more suitable term would be circular or annular waves. Due to the interaction of random boundaries, the system exhibits

planar waves, irregular curved waves, and other patterns. However, this circular wave is unstable and can vary with time and random boundaries. Previous studies have shown that when neurons are in spiking state, the system is more prone to spiral waves, and the coupling strength range for spiral waves is wider. When neurons are in period-2 bursting or other states, the system can only generate spiral waves when the initial phase distribution of neurons is relatively uniform.

The influence of the change in control parameter k on the spiral wave in the two-dimensional network is also worth studying, as shown in Figure 10. As $1/k$ represents the parameter related to the calcium ion exchange rate, therefore it affects the fast variable y by changing the newly introduced variable w, and ultimately regulates the membrane potential of neuron. Under the selected parameter conditions, the change in the value of k has a certain impact on the formation of spiral waves in two-dimensional networks, but this effect is relatively limited. When the value of k is greater than 60, obvious spiral wave arms can be observed in the four corners of the two-dimensional lattice, and the direction of rotation of its wave head is also changing. In all cases, the lattice can only generate wavelets, ultimately forming a square wave propagating towards the center, known as an anti-target wave or circular waves. It can be inferred that the neurons are in period-2 bursting state at this time from this phenomenon.

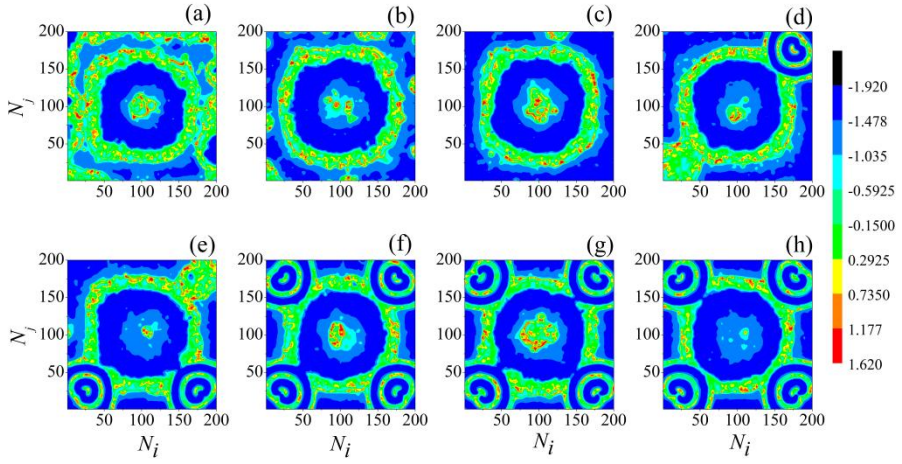

Figure 10. Development of spiral wave induced by random values of boundary at different control parameter k with $D = 0.5$, $I_{ext} = 1.9$ at $t = 20000$ time units. (a)-(h) $k = 10, 20, 30, 50, 55, 60, 90, 100$. The change in the value of control parameter k has a certain impact on the formation of spiral waves in two-dimensional networks, and if the value of control parameter k is greater than 60, the spatiotemporal pattern of the system does not change much.

3.3 Synchronization factor of the network

In order to detect the collective behavior of neurons in the two-dimensional network, the synchronization factor R are calculated in Figures 11-13. As is known to all that the synchronization factor of the network in a uniform state is relatively high. If the network presents an ordered state, the synchronization factor is small. The distribution of synchronization factors can effectively distinguish the generation types of different target waves.

It can be clearly observed that as the control parameter k and coupling intensity D increase, the synchronization factor R shows a monotonic decreasing trend, suggesting that relatively smaller values of k and D correspond to larger synchronization factors. Although both Figures 11 and 12 are all monotonically decreasing curves, there are still differences if compare both of them. If the value of k

is greater than 60, it has almost no impact on the synchronization factor, which can also be concluded in Figure 10. When the coupling strength D is greater than 0.2, it can be seen that increasing the coupling strength does not affect the synchronization factor R, and the spiral wave pattern changes in the system are not significant, as shown in Figure 12.

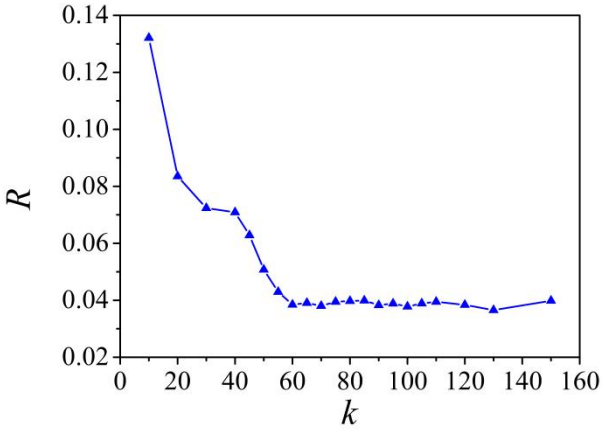

Figure 11. Synchronization factor R varies with different control parameter k. Synchronization factor varies with control parameter shows monotonically decreasing curve.

The influence of external stimulus intensity on synchronization factors has characteristics similar to multiple resonances. It can be intuitively seen that as the intensity of external stimulation current increases, the synchronization factor R gradually decreases first, and then R drops to 0 at I_{ext} = 1.3. Subsequently, the synchronization factor R value shows fluctuating changes, and three maximum values can be observed. These conclusions are basically consistent with Figure 7, I_{ext} = 1.3 is a critical point for the system to undergo phase transition, which determines whether the neuron is in quiescent or discharging state.

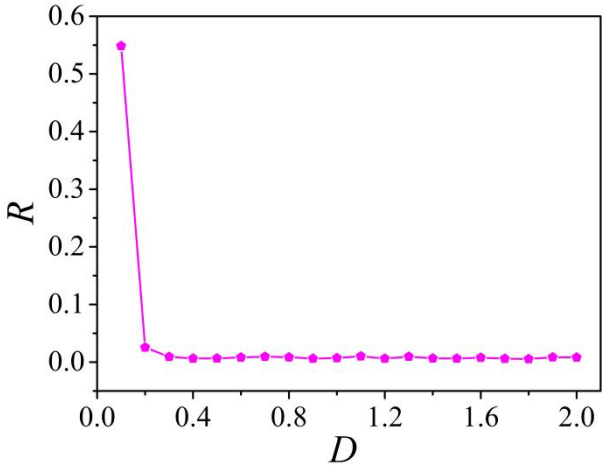

Figure 12. Synchronization factor R varies with coupling intensity D. Synchronization factor varies with coupling intensity shows monotonically decreasing curve.

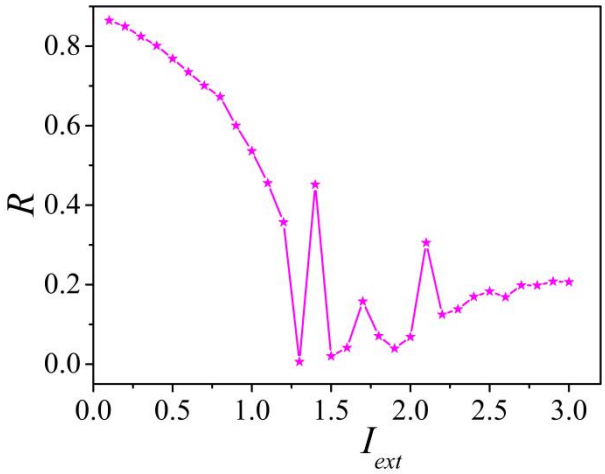

Figure 13. Synchronization factor R varies with external stimulus intensity I_{ext}. As the intensity of external stimulation current increases, the synchronization factor R shows fluctuating changes.

4. Conclusions

Considering the limitations of typical three-variable HR neural model in describing the complex nonlinear characteristics and precise behavioral patterns, a new variable is introduced into the classic HR neural model to analyze the discharge characteristics and bifurcation behavior of the modified HR model. The influence of the control parameter of the new variable on the extended HR neuronal membrane potential is explored, and the evolutionary relationship between the new variable and other variables are investigated as well. It is found that the discharge characteristics of the system are more diverse due to the newly introduced variable, and the appearance of multimodality can be observed.

The spatiotemporal dynamics of two-dimensional lattice was also explored by using the induction of random boundary functions, and the formation and breakup mechanisms of spiral waves in the two-dimensional network were explored. At the same time, the synchronization characteristics of the network were also analyzed by calculating the synchronization factor. It is found that if the number of spikes in neuronal bursting is small, the wave arm of the spiral wave is thinner, resulting in a smaller size and larger number of spiral waves, and there is no single spiral wave in the lattice. If the number of peaks in neuronal bursting increases, the spiral wave arm becomes thicker, and the size of the spiral wave in the lattice becomes larger and the number correspondingly decreases. It is concluded that the synchronization factor R show a monotonic decreasing trend with the increasing of the control parameter k and coupling intensity D.

The above results are helpful in understanding how spiral waves spontaneously form in the cerebral cortex, especially in understanding the mechanism of epilepsy, as epilepsy is a functional brain disorder caused by the synchronization of a large number of neurons. These results can answer how synchronous oscillations are generated, and the formation mechanism of oscillatory death of a large number of neurons also provides useful information for the treatment of epilepsy.

Acknowledgments

This work is supported by the Jiangxi Provincial Natural Science Foundation of China, the Natural Science Foundation of Jiangxi Provincial Department of Education (No. GJJ2202903,

GJJ210841), and the Special Fund for Doctoral Talent Introduction Project of Nanchang Institute of Science and Technology (No. NGRCZX-22-07).

Author Contributions

Yan Fu: Writing-Original draft preparation, Supervision, Data curation, Validation, Software; **Guowei Wang**: Software, Conceptualization, Visualization, Methodology, Investigation, Writing-Reviewing and Editing.

Data availability statement

The authors confirm that the data supporting the findings of this study are available within the article.

Conflict of interest

The authors declare there is no conflict of interest.

References

1. Pashaei A, Bayer J, Meillet V, et al. (2015) Computation and projection of spiral wave trajectories during atrial fibrillation: a computational study. *Cardiac electrophysiology clinics*, 7(1): 37-47. https://doi.org/10.1016/j.ccep.2014.11.001
2. Wu FQ, Wang RB. (2023) Synchronization in memristive HR neurons with hidden coexisting firing and lower energy under electrical and magnetic coupling. *Commun Nonlinear SCI*, 126(11): 107459. https://doi.org/10.1016/j.cnsns.2023.107459
3. Wang GW, Ge MY, Lu LL, et al. (2021) Study on propagation efficiency and fidelity of subthreshold signal in feed-forward hybrid neural network under electromagnetic radiation. *Nonlinear Dynam*, 103(3): 2627-2643. https://doi.org/10.1007/s11071-021-06247-z
4. Mohammad BJ, Mahdi RK. (2022) The effects of temperature on the dynamics of the biological neural network. *J Biol Phys*, 48(1): 111-126. https://doi.org/10.1007/s10867-021-09598-1
5. Bao BC, Hu JT, Cai JM, et al. (2023) Memristor-induced mode transitions and extreme multistability in a map-based neuron model. *Nonlinear Dynam*, 111(4): 3765-3779. https://doi.org/10.1007/s11071-022-07981-8
6. Li F, Li XL, Ren LQ. (2022) Noise-induced collective dynamics in the small-world network of photosensitive neurons. *J Biol Phys*, 48(3): 321-338. https://doi.org/10.1007/s10867-022-09610-2
7. Bessa WM, Lima GDS. (2022) Intelligent control of seizure-like activity in a memristive neuromorphic circuit based on the Hodgkin-Huxley model. *J Low Power Electron App*, 12(54): 12040054. https://doi.org/10.3390/jlpea12040054
8. Vivekanandhan G, Hamarash II, Ali Ali AM, et al. (2022) Firing patterns of Izhikevich neuron model under electric field and its synchronization patterns. *Eur Phys J Spec Top*, 231(22): 4017-4023. https://doi.org/10.1140/epjs/s11734-022-00636-0

9. Kabilan1 R, Venkatesan A. (2023) Vibrational resonance in a damped bi-harmonic driven mathews -lakshmanan oscillator. *J Vib Eng Technol*, 11(2): 897-903. https://doi.org/10.1007/s42417-023-00897-6
10. Chen L, Campbell SA. (2022) Exact mean-field models for spiking neural networks with adaptation. *J Comput Neurosci*, 50(4): 445-469. https://doi.org/10.1007/s10827-022-00825-9
11. Yu D, Wang GW, Ding QM, et al. (2022) Effects of bounded noise and time delay on signal transmission in excitable neural networks. *Chaos Solitons Fract*, 157, 111929. https://doi.org/10.1016/j.chaos.2022.111929
12. Zhou XY, Xu Y, Wang GW, et al. (2020) Ionic channel blockage in stochastic Hodgkin-Huxley neuronal model driven by multiple oscillatory signals. *Cogn Neurodynamics*, 14(4): 569-578. https://doi.org/10.1007/s11571-020-09593-7
13. Lu LL, Gao ZH, Wei ZC, et al. (2023) Working memory depends on the excitatory- inhibitory balance in neuron-astrocyte network. *Chaos*, 33(1): 013127. https://doi.org/10.3389/fnmol.2021.689952
14. Khouhak J, Faghani Z, Jafari S. (2019) Wave propagation in a network of interacting nephrons. *Physica A*, 530(9): 121566. https://doi.org/10.1016/j.physa.2019.121566
15. Weise LD, Panfilov AV. (2019) Mechanism for mechanical wave break in the heart muscle. *Physi Rev Lett*, 119(9): 108101. https://doi.org/10.1103/PhysRevLett.119.108101
16. Jakubith S, Rotermund HH, Engel W, et al. (1990) Spatiotemporal concentration patterns in a surface reaction: Propagating and standing waves, rotating spirals, and turbulence. *Physi Rev Lett*, 65(24): 3013. https://doi.org/10.1103/PhysRevLett.65.3013
17. Sandeep K, Amita D. (2018) Spiral waves in driven strongly coupled Yukawa systems. *Phys Rev E*, 97(6): 063202. https://doi.org/10.1103/PhysRevE.97.063202
18. He SB, Rajagopal K, Karthikeyan A, et al. (2023) A discrete Huber-Braun neuron model: from nodal properties to network performance. *Cogn Neurodynamics*, 17(1): 301-310. https://doi.org/10.1007/s11571-022-09806-1
19. Rajeshkanna S, Hayder N, Karthikeyan R, et al. (2023) The dynamic analysis of discrete fractional-order two-gene map. *Eur Phys J Spec Top*, https://doi.org/10.1140/epjs/s11734-023-00912-7.
20. Zhdanov VP. (2019) Spatio-temporal aspects of the interplay of cancer and the immune system. *J Biol Phys*, 45(4): 395-400. 10.1007/s10867-019-09535-3
21. Wang GW, Xu Y, Ge MY, et al. (2020) Mode transition and energy dependence of FitzHugh - Nagumo neural model driven by high-low frequency electromagnetic radiation. *AEU - Int J Electron C*, 120: 153209. https://doi.org/10.1016/j.aeue.2020.153209
22. Ge MY, Wang GW, Jia Y. (2021) Influence of the Gaussian colored noise and electromagnetic radiation on the propagation of subthreshold signals in feedforward neural networks. *Sci China Technol Sci*, 64(4): 847-857. https://doi.org/10.1007/s11431-020-1696-8
23. Ding QM, Wu Y, Hu YP. (2023) Tracing the elimination of reentry spiral waves in defibrillation. *Chaos Solitons Fract*, 174(7): 113760. https://doi.org/10.1016/j.chaos.2023.113760
24. Shepelev IA, Muni SS, Vadivasova TE. (2021) Synchronization of wave structures in a heterogeneous multiplex network of 2D lattices with attractive and repulsive intra-layer coupling. *Chaos*, 31(2): 021104. https://doi.org/10.1016/10.1063/5.0044327

25. Bukh A, Strelkova G, Anishchenko V. (2019) Spiral wave patterns in a two-dimensional lattice of nonlocally coupled maps modeling neural activity. *Chaos Solitons Fract*, 120: 75-82. https://doi.org/10.1016/j.chaos.2018.11.037
26. Etémé AS, Tabi CB, Mohamadou A, et al. (2019) Elimination of spiral waves in a two-dimensional Hindmarsh-Rose neural network under long-range interaction effect and frequency excitation. *Physica A*, 533: 122037. https://doi.org/10.1016/j.physa.2019.122037
27. Nayak AR, Pandit R. (2014) Spiral-wave dynamics in ionically realistic mathematical models for human ventricular tissue: the effects of periodic deformation. *Front Physiol*, 5, 207. https://doi.org/10.3389/fphys.2014.00207
28. Bukh AV, Schöll E, Anishchenko VS. (2019) Synchronization of spiral wave patterns in two-layer 2D lattices of nonlocally coupled discrete oscillators. *Chaos*, 29(5): 053105. https://doi.org/10.1063/1.5092352
29. Wu Y, Ding QM, Yu D, et al. (2022) Pattern formation induced by gradient field coupling in bi-layer neuronal networks. *Eur Phys J Spec Top*, 231(22): 4077-4088. https://doi.org/10.1140/epjs/s11734-022-00628-0
30. Yao YG, Deng HY, Ma CZ, et al. (2017) Impact of bounded noise and rewiring on the formation and instability of spiral waves in a Small-World network of Hodgkin-Huxley neurons. *PLoS ONE* , 12(1): e0171273. https://doi.org/10.1371/journal.pone.0171273
31. Wang GW, Fu Y. (2023) Spatiotemporal patterns and collective dynamics of bi-layer coupled Izhikevich neural networks with multi-area channels. *Math Biosci Eng*, 20(2): 3944-3969. https://doi.org/10.3934/mbe.2023184
32. Luo H, Ma J. (2020) Dynamic behaviors of spiral waves in cardiac tissue under electromagnetic radiation. *AIP Advances*, 10(5): 055101. https://doi.org/10.1063/5.0003109
33. Hindmarsh JL, Rose RM. (1984) A model of neuronal bursting using three coupled first order differential equations. *P Roy Soc B: Biol Sci*, 221(1222): 87-102. https://doi.org/10.1098/rspb.1984.0024
34. Rajagopal K, Karthikeyan A, Jafari S, et al. (2020) Wave propagation and spiral wave formation in a Hindmarsh–Rose neuron model with fractional-order threshold memristor synaps. *Internat J Mod Phys B*, 34(17): 2050157. https://doi.org/10.1142/S021797922050157X
35. Hayati M, Nouri M, Abbott D, et al. (2016) Digital multiplierless realization of two-coupled biological Hindmarsh-Rose neuron model. *IEEE T Circuits II*, 63(5): 463-467. https://doi.org/10.1109/TCSII.2015.2505258
36. Xu Y, Wang CN, Jin WY, et al. (2015) Investigation of emergence of target wave and spiral wave in neuronal network induced by gradient coupling. *Acta Phys Sin*, 64(19): 198701.
37. Ma J, Song XL, Tang J, et al. (2015) Wave emitting and propagation induced by autapse in a forward feedback neuronal network. *Neurocomputing*, 167(1): 378-389. https://doi.org/10.1016/j.neucom.2015.04.056
38. Torrealdea FJ, D'Anjou A, Graña M. (2006) Energy aspects of the synchronization of model neurons. *Phys Rev E*, 74: 011905. https://doi.org/10.1103/PhysRevE.74.011905
39. Wang GW, Yu D, Ding QM, et al. (2021) Effects of electric field on multiple vibrational resonances in Hindmarsh-Rose neuronal systems. *Chaos Solitons Fract*, 150: 111210. https://doi.org/10.1016/j.chaos.2021.111210

40. Vijay SD, Thamilmaran K, Ahamed AI. (2023) Superextreme spiking oscillations and multistability in a memristor-based Hindmarsh-Rose neuron model. *Nonlinear Dynam*, 111(1): 789-799. https://doi.org/10.1007/s11071-022-07850-4
41. Lu LL, Yi M, Gao ZH, et al. (2023) Critical state of energy-efficient firing patterns with different bursting kinetics in temperature-sensitive Chay neuron. *Nonlinear Dynam*, Doi:10.1007/s11071-023-08700-7.
42. Wang GW, Yang LJ, Zhan X, et al. (2022) Chaotic resonance in Izhikevich neural network motifs under electromagnetic induction. *Nonlinear Dynam*, 107(4): 3945-3962. https://doi.org/10.1007/s11071-021-07150-3
43. Qiao S, An XL. (2021) Dynamic response of the e-HR neuron model under electromagnetic induction. *Pramana-J Phys*, 95(2): 72. https://doi.org/10.1007/s12043-021-02095-z
44. Rajagopal K, Khalaf AJM, Parastesh F, et al. (2019) Dynamical behavior and network analysis of an extended Hindmarsh-Rose neuron model. *Nonlinear Dynam*, 98(12): 477-487. https://doi.org/10.1007/s11071-019-05205-0
45. Hou ZL, Ma J, Zhan X, et al. (2020) Estimate the electrical activity in a neuron under depolarization field. *Chaos Solitons Fract*, 142(4): 110522. https://doi.org/10.1016/j.chaos.2020.110522
46. Wang GW, Fu Y. (2023) Modes transition and network synchronization in extended Hindmarsh-Rose model driven by mutation of adaptation current under effects of electric field. *Indian J Phys*, 97(8): 2327-2337. https://doi.org/10.1007/s12648-023-02613-2
47. Wu Y, Wang B, Zhang X, et al. (2019) Spiral wave of a two-layer coupling neuronal network with multi-area channels. *Int J Mod Phys B*, 33(29): 1950354. https://doi.org/10.1142/S0217979219503545
48. Wang GW, Wu Y, Xiao FL, et al. (2022) Non-Gaussian noise and autapse-induced inverse stochastic resonance in bistable Izhikevich neural system under electromagnetic induction. *Physica A*, 598: 127274. https://doi.org/10.1016/j.physa.2022.127274
49. Li TY, Wang GW, Yu D, et al. (2022) Synchronization mode transitions induced by chaos in modified Morris-Lecar neural systems with weak coupling. *Nonlinear Dynam*, 108(3): 2611-2625. https://doi.org/10.1007/s11071-022-07318-5
50. Serrano F, Ghosh D. (2022) Sliding mode synchronization of complex resonant Josephson junction network. *Eur Phys J Spec Top*, 231(22), 3999-4006. https://doi.org/10.1140/epjs/s11734-022-00695-3
51. Medvedeva TM, Lüttjohann AK, Sysoeva MV, et al. (2020) Estimating complexity of spike-wave discharges with largest Lyapunov exponent in computational models and experimental data. *AIMS Biophys*, 7(2): 65-75. https://doi.org/10.3934/biophy.2020006
52. Francisco JT, Cecilia S, Alicia DA, et al. (2009) Energy efficiency of information transmission by electrically coupled neurons. *BioSystems*, 97(1): 60-71. https://doi.org/10.1016/j.biosystems.2009.04.004
53. Into A, Vesa K. (2023) Similarity of epidemic spreading and information network connectivity mechanisms demonstrated by analysis of two probabilistic models. *AIMS Biophys*, 10(2): 173-183. https://doi.org/10.3934/biophy.2023011
54. Yu D, Zhou XY, Wang GW, et al. (2022) Effects of chaotic activity and time delay on signal transmission in FitzHugh-Nagumo neuronal system. *Cogn Neurodynamics*, 16(4): 887-897. https://doi.org/10.1007/s11571-021-09743-5

564 55. Mahamad IK, Laxmikanth SM, Tarika G, et al. (2022) Artificial intelligence and 3D printing
565 technology in orthodontics: future and scope. *AIMS Biophys*, 9(3): 182-197.
566 https://doi.org/10.3934/biophy.2022016
567 56. Mohammad SF, Abdolsamad H. (2023) Dynamical response of autaptic Izhikevich neuron
568 disturbed by Gaussian white noise. *J Comput Neurosci*, 51(1): 59-69.
569 https://doi.org/10.1007/s10827-022-00832-w
570 57. Natarajan M, Arumugam V, Jehad A. (2023) Passivity analysis for Markovian jumping neutral
571 type neural networks with leakage and mode-dependent delay. *AIMS Biophys*, 10(2): 184-204.
572 58. Yu D, Lu LL, Wang GW, et al. (2021) Synchronization mode transition induced by bounded
573 noise in multiple time-delays coupled FitzHugh-Nagumo model. *Chaos Solitons Fract*, 147:
574 111000. https://doi.org/10.1016/j.chaos.2021.111000
575

576 AIMS Press
577